

Interior ballistic two-phase flow model of guided-projectile gun system utilizing stick propellant charge

MAHMOUD RASHAD

School of Energy and Power Engineering
Nanjing University of Science and Technology
Xiaolingwei, 200 Nanjing, Jiangsu Province
CHINA

XIAOBING ZHANG

School of Energy and Power Engineering
Nanjing University of Science and Technology
Xiaolingwei, 200 Nanjing, Jiangsu Province
CHINA

HAZEM ELSADEK

School of Energy and Power Engineering
Nanjing University of Science and Technology
Xiaolingwei, 200 Nanjing, Jiangsu Province
CHINA

mahmodmosa2004@yahoo.com

Abstract:- Launching a guided projectile from conventional artillery is a very sensitive process for both the propelling charge and the gun system. Hence, a specific mathematical model based on two-phase fluid dynamics of solid single-perforated high density stick propellant and its products of combustion inside the gun tube during interior ballistics cycle is developed. The model includes the governing equations of mass, momentum and energy for both phases as well as the constitutive laws. The simulations are applied to conventional large caliber naval gun firing a guided projectile. The results are compared with the experimental data of granular propellant grains for validation. Different stick propellant grain design parameters are investigated. The grain size significantly affected the maximum chamber pressure and then the guided projectile muzzle velocity. An appropriate stick grain size condition exists, where the minimum pressure wave generation can be obtained. Based on the simulation results, an apparent guideline for the proper design of stick propellant charge for launching guided projectiles is presented.

Key-Words:- Stick propellant, Two-phase flow, Interior ballistics, Guided-projectile

1 Introduction

Employing guided projectiles with conventional artillery has three crucial benefits which they are; (1) increasing the accuracy that guarantees target damage, (2) far fewer rounds are needed to destroy the target, (3) cost savings for establishment of modern artillery systems, and (4) an order-of-magnitude reduction in the logistics train behind the artillery unit. However, these projectiles utilize a variety of electronic and electromechanical devices for fusing, target detection, guidance and control. Consequently, these sensitive versions of munitions

require more precise interior ballistic loading conditions and accurate propelling charge designs in order to survive against harsh environment inside the gun. At the same time, the propulsion system must get the projectile through the launch environment with consistent muzzle velocities, but without excessive stresses to gun chamber or the projectile. The projectile muzzle velocity is one of the key parameters of the gun performance, which is constrained by the maximum chamber pressure during the ballistic cycle. The permissible value of maximum pressure is usually controlled by gun tube design, but distant from this maximum value, the

pressure profile applied on the projectile base is a result of the amount of gases produced by the burned propellant. At the beginning of combustion process, the projectile is not moving or just has a very slow movement, so the chamber pressure rises rapidly as the propellant continues to burn. Consequently, high pressurized gases accelerate the projectile down the bore, as a result the free volume behind the projectile increases much faster than gases are produced to fill it. Accordingly, the pressure possesses a very rapid decline much more required. Therefore, maximizing propellant energy, loading density, and progressivity of gas production (continuous increase in burning surface) are the major considerations for enhancing conventional gun performance that guarantee safe launching for guided munitions with the necessary muzzle velocity.

Lumped parameters models are usually enough to predict the gun performance to some extent in such cases where conventional projectiles are launched, [1, 2]. Conversely, the guided munitions require more precise two-phase flow models to explain the complex phenomena occur in a gun chamber during the whole interior ballistic cycle. The authors' interior ballistics research group developed many two-phase flow models to study different propelling charge configurations revealing a progressive burning such as; 7- or 19-Perforated (7-P, 19-P) grains to launch a guided projectile [3-9]. Results of these studies were in a good agreement with the experimental data. However, during these studies a high pressure waves disturbing projectile base were recorded. In order to protect the guided projectile against these pressure waves, the shell safety has to be increased which leads to an increase in projectile weight at the expense of its intended destructive capability. Design of a proper stick propellant charge is another more sophisticated approach to overcome this problem. Some numerical simulations for gun systems of small to large caliber launching conventional projectiles employed stick propellant instead of the granular solid propellant grains [10-12]. Although these studies went through realistic investigations of the complex two-phase flow phenomena inside gun chamber, it did not address the ballistic problem of stick propellant charges launching a guided projectile.

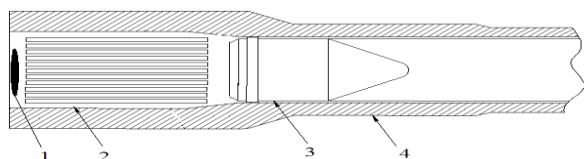
Therefore, the objectives of this research work is to develop a strict mathematical model based on two-phase fluid dynamics of solid single-perforated stick propellant and its products of combustion inside the gun tube during interior ballistics cycle of conventional large caliber naval gun firing a guided

projectile. The simulation results of single-perforated stick propellant grain shape are compared to that obtained from the previous work for granular propellant grains [3-9]. It is intended, using this model, to design charges more convenient for launching process of guided projectiles at a high muzzle velocity without increasing the maximum pressure exerted on both gun chamber and the guided projectile.

2 Physical model and underlying assumptions

Figure 1 represents schematically the configuration of a typical bundle of single-perforated stick propellant charge utilized to launch a guided projectile in a conventional naval large caliber gun. The solid propellant is loaded distant from the breech and the projectile base by a certain distance depending on the charge design parameters, e.g. stick length. The sequence of physical events may summarize as follows; the igniter is actuated mechanically or electrically. Hot gas flows from the igniter into the primer charge. This creates a process of convective burning within the granular primer charge. The hot gas from the igniter preheats grains of black powder which ignite and contribute more hot gas for the ignition of other grains of black powder. The hot primer gas rushes over the outer and inner surfaces of the propellant sticks and heats them through the mechanisms of conduction, radiation and convection with the latter playing the principal role [13]. The combustion process rapidity is promoted by the convectively driven inert heating, and by the growing chamber pressure. The burning process of the propelling charge continues under the convective heating condition depending on two major factors, the dynamics and temperature of the primer gas and the degree of progressivity of sticks. Subsequently, the whole propellant bundle is ignited and the phenomenon of flame spreading is ended. The criterion of ignition, flame spreading and combustion of stick propellant grains can be also referred to [14]. The projectile's rotating band starts to engrave into the rifling of the tube as the forces exerted on the projectile base by the combustion gas increases sufficiently. Once ignition of the entire charge has occurred, the pressure build up in the chamber very rapidly. Eventually, sufficient pressure is reached to completely overcome driving band engraving resistance and the projectile rapidly accelerates down the bore until it expels out the gun muzzle. One of the major advantages of the used charge configuration is that the flame resistance through the charge of a stick

propellant bundle is lower than that through granular propellants packed beds [15].



1. Primer and igniter, 2. Stick propellant bundle, 3. guided projectile, 4. barrel.

Fig. 1 Schematic illustration of stick propellant charge in conventional large caliber gun.

To simplify modeling of the physical events occurring during this complex interior ballistic process of combustion of single-perforated stick propellant charge, some basic assumptions are developed as:

- Stick propellants are assumed not to break or bend, and are also assumed to move in the axial direction only and the motion of the propellant is described by Lagrange method, ignoring the turbulent viscosity and dissipation.
- Burning in the inner and outer surfaces of a stick is axisymmetric.
- Stick propellant torsion or rotation during movement or compaction by the effect of combustion gases is negligible.
- There are no body forces.
- Propellant density is constant.
- Burning process of the stick ends is uniform.
- Each local part across the computational domain of the stick propellant is assumed to burn according to the ambient pressure at that local position.
- Gases obey Nobel-Abel equation of state ignoring the viscous dissipation and heat loss to the gun barrel.
- The initial geometrical parameters and physical conditions of the stick propellants are the same. Additionally, to simplify the mathematical formulation, the combustion of stick in a bundle is represented by a single stick.

3 Mathematical model

3.1 Basic equations

Transient gas-dynamical behavior of hot gas penetration, flame propagation, gun chamber pressurization, and combustion process of stick propellant is comprehensively explained by driving the mass, momentum, and energy equations for the gas-phase as well as the mass and momentum

equations for the solid-phase. The governing equations are approached by considering the balance of fluxes over a control volume small enough to give the desired spatial distribution in the complete system but large enough to contain many solid particles [16]. The developed two-phase flow model has the capability of explanation the interaction between the gas-phase and solid-phase via adding the source term to the single-phase conservation laws. The mathematical model of stick propellant charge is quite different from that of granular propellant [3-9]. Based on the above assumptions, the basic equations are as follows:

Gas-phase mass equation

$$\frac{\partial(\varphi\rho_g A)}{\partial t} + \frac{\partial(\varphi\rho_g u_g A)}{\partial x} = \dot{m}_c A \tag{1}$$

Gas-phase momentum equation

$$\begin{aligned} \frac{\partial(\varphi\rho_g u_g A)}{\partial t} + \frac{\partial(\varphi\rho_g u_g^2 A)}{\partial x} + A\varphi \frac{\partial p}{\partial x} \\ = -f_s A + \dot{m}_c u_p A \end{aligned} \tag{2}$$

Gas-phase energy equation

$$\begin{aligned} \frac{\partial[\varphi\rho_g (e_g + \frac{u_g^2}{2})A]}{\partial t} + \frac{\partial[\varphi\rho_g u_g (e_g + \frac{u_g^2}{2} + \frac{p}{\rho_g})A]}{\partial x} \\ + p \frac{\partial(A\varphi)}{\partial t} = -Q_p A - f_s u_p A + \dot{m}_c (e_p + \frac{u_p^2}{2} + \frac{p}{\rho_p})A \end{aligned} \tag{3}$$

Solid-phase mass equation

$$\frac{\partial(\varphi_p \rho_p A)}{\partial t} + u_p \frac{\partial(\varphi_p \rho_p A)}{\partial x} = -\dot{m}_c A \tag{4}$$

Where, A is the gun tube cross section area, φ is the volume fraction of the gas-phase, φ_p is the volume fraction of the solid phase, ρ_g, ρ_p are gas and solid density, u_g, u_p are gas and solid phase velocity, P, e_g are pressure and internal energy of the gas-phase, m_c is the rate of gas mass generation due to propellant combustion, f_s, Q_p are interphase drag and interphase heat transfer, respectively.

Solid-phase momentum conservation equation

Considering the role of the differential pressure as well as interphase drag across the stick propellant surface, the solid-phase momentum equation can be written as follows:

Where, the weighting factor, k , has limited values which cannot be too small to prevent results fluctuations.

$$\begin{aligned} & \frac{d}{dt} \int_{x_L}^{x_R} \varphi_p \rho_p u_p A dx \\ &= A(1-\varphi)p|_b - A(1-\varphi)p|_f \\ & - \int_{x_L}^{x_R} \dot{m}_c u_p A dx + \int_{x_L}^{x_R} A f_s dx \end{aligned} \quad (5)$$

Where, the subscripts b and f refer to the bottom and the front end of the stick propellants, respectively. While, the coordinate values x_L, x_R for the left and the right ends of the stick propellants respectively, and satisfies:

$$\frac{dx_L}{dt} = u_p, \quad \frac{dx_R}{dt} = u_p \quad (6)$$

3.2 Constitutive relations

Constitutive relations are needed to close the preceding governing equations above and express the interaction between the two phases such as gas equation of state, interphase drag, and interphase heat transfer.

a. The Gas satisfies the Abel-Noble equation of state [17]:

$$p = \frac{RT_g}{\left(\frac{1}{\rho_g} - \alpha\right)} \quad (7)$$

Where, R is the gas constant, T_g is the gas temperature, and α is the gas co-volume.

b. Interphase drag

The flow resistance of stick propellant is lower than that of granular propellant grains, according to the experimental results presented in [15]. When the porosity of the sticks under the same conditions as the granular propellant grains taking value less than or equal to 0.6, the friction coefficient was found to be 0.17; when the porosity has a value of $\phi \geq 0.8$ then, the coefficient of friction is equal to 0.018; for ϕ within the range of (0.6 - 0.8) the friction coefficient is calculated by linear interpolation. So, the Interphase drag of the stick can be calculated as follows:

$$\begin{aligned} f_s &= \frac{1-\phi}{d_p} |u_g - u_p| (u_g - u_p) \rho_g \Pi \\ \Pi &= \begin{cases} 0.17 & \phi \leq 0.6 \\ 0.17 - 0.152(\phi - 0.6)/0.2 & 0.6 < \phi \leq 0.8 \\ 0.018 & 0.8 < \phi \leq 1 \end{cases} \end{aligned} \quad (8)$$

c. Interphase heat transfer

$$\begin{aligned} Q_p &= \rho_p (1-\phi) S_p q / M_p \\ S_p &= \sigma S_i \\ M_p &= (1-\psi) M_i \end{aligned} \quad (9)$$

Where, σ, ψ are the propellant's relative burned surface ratio and the propellant's relative burned quantity, they can be determined from the shape function relations for stick propellant, respectively, and S_i, M_i are the initial burning surface and mass of a propellant sticks, respectively.

Considering the two forms of convection and radiation, interphase heat exchange q is calculated as [10]:

$$\begin{aligned} q &= (h_p + h_{re})(T_g - T_{ps}) \\ h_p &= 0.4 \text{Re}_p^{2/3} Pr^{1/3} \lambda_f / d_p, \quad Pr = \frac{4\gamma}{9\gamma - 5} \\ \text{Re}_p &= d_p \rho_g |u_p - u_g| / \mu \\ \mu &= C_1 T_g^{3/2} / (C_2 + T_g) \\ \lambda_f &= C_3 T_g^{3/2} / (C_4 + T_g) \\ h_{re} &= C_5 (T_g + T_{ps})(T_g^2 + T_{ps}^2) \end{aligned} \quad (10)$$

Where, h_p is the heat transferred by convection, h_{re} is the heat transferred by radiation, T_{ps} is the solid particle surface temperature, Re_p is the Reynolds number, λ_f is the thermal transfer coefficient, μ is the molecular viscosity, and γ is the specific heat ratio.

d. Particle surface temperature

Considering that the ignition process of stick propellant is uniform incident, the particle surface temperature can be expressed as:

$$\frac{dT_{ps}}{dt} = \frac{2q \sqrt{a_p}}{\lambda_p \sqrt{\pi}} \frac{(\sqrt{t+\delta t} - \sqrt{t})}{\delta t} \quad (11)$$

Where, a_p is the acceleration of propellant particles, and λ_p is the coefficient of conductivity.

e. The rate of gas mass generation due to propellant combustion is calculated depending on the propellant burning rate equation as follows:

$$\begin{aligned} \frac{dr_p}{dt} &= -\dot{d} \\ \dot{d} &= bp^n \\ \dot{m}_c &= \rho_p^2(1-\phi)S_p\dot{d} / M_p \end{aligned} \quad (12)$$

Where, b is the burning rate coefficient, n is the burning rate exponent.

f. Stick propellant grain shape function

Figure 2 is a simple schematic representing the main design parameters of the stick propellant grain with magnified cross-section. Where, R is the outer radius of the stick, r is the perforation radius, e_1 is the half web thickness and c is the stick length.

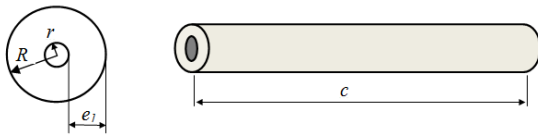


Fig. 2 The schematic illustration of the stick propellant grain shape parameters.

The shape functions of the stick propellant grain used in this study is developed as:

$$\begin{cases} \psi = \chi Z(1 + 2\lambda Z + 3\mu Z^2) \\ \sigma = 1 + 2\lambda Z + 3\mu Z^2 \end{cases} \quad (13)$$

$$\chi = 1 + \beta, \quad \lambda = -\left(\frac{\beta}{1 + \beta}\right), \quad \beta = \frac{e_1}{c}$$

Where, Z is the relative burned thickness of the stick propellant grain

4 Numerical approach

The input data for computations carried out by the code is given in Table 1, while the main characteristics of the used stick propellant charge is presented in Table 2 Equations (1-4) can be written in the form of conservation laws for simplifying the numerical solution:

$$\frac{\partial U}{\partial t} + \frac{\partial F}{\partial x} = H \quad (14)$$

Where,

$$U = \begin{bmatrix} \phi \rho_g A \\ \phi \rho_g u_g A \\ \phi \rho_g A \left(e_g + \frac{u_g^2}{2} \right) \\ (1 - \phi) \rho_p A \end{bmatrix}, \quad F = \begin{bmatrix} \phi \rho_g u_g A \\ \phi \rho_g (u_g^2 + P) A \\ \phi \rho_g U_g A \left(e_g + \frac{u_g^2}{2} + \frac{P}{\rho_g} \right) \\ (1 - \phi) \rho_p u_p A \end{bmatrix}$$

$$, H = \begin{bmatrix} \dot{m}_c A \\ -f_s A + \dot{m}_c u_p A + p \frac{\partial(A\phi)}{\partial x} \\ -f_s u_p A - Q_p + \dot{m}_c A \left(e_p + \frac{p}{\rho_p} + \frac{u_p^2}{2} \right) - p \frac{\partial(\phi A)}{\partial t} \\ -\dot{m}_c A \end{bmatrix}$$

The nonlinear hyperbolic system of differential equations of the established two-phase reactive flow model is solved using Maccromack's technique which is an explicit finite difference method with second order accurate in both space and time via two steps, predictor and corrector with the prescribed CFL stability condition same as applied in [5, 18]. The solid-phase momentum equation, Eq.(5), is solved using integration methods. The moving control volume conservation method is used to handle the moving boundary as well as a self-adapting method was used to expand the computational domain in order to follow the projectile motion as described in [5, 8].

Table 1 Characteristics of guide-projectile conventional gun system.

Parameter	Value
Gun caliber (m)	0.130
Barrel length (m)	6.29
Chamber length (m)	0.7
Chamber volume (m ³)	0.01366
Projectile mass (Kg)	33.4

Table 2 Characteristics of solid stick propellant.

Parameter	Value
Shape of grain	Cylindrical with one perforation
Grain dimensions (mm)	$\phi 5.5 \sim \phi 8 \times 400 \sim 600$
Perforation diameter (mm)	2.2 ~ 4
Propellant charge mass (Kg)	10.6
Propellant co-volume (m ³ /kg)	0.001
Propellant density (kg/m ³)	1650
Propellant force (J/kg)	1226000
Specific heat ratio γ	1.22
Initial porosity	0.54
Burning rate coefficient	$1.7e10^{-9}$
Burning rate exponent	0.92

5 Simulation results and discussions

5.1 Application of the model to guided-projectile gun system

The developed two-phase flow model in this study is applied to conventional naval gun launching a guided projectile utilizing single-perforated stick propellant charge shown in Fig.1. Figure 3 represents the z-t contour diagrams with the distributions of (a) pressure, (b) gas temperature, (c) gas velocity, and (d) porosity. This results are at a representative stick propellant grain conditions of; $c = 500mm$, $R = 4mm$ and $r = 1.1mm$ and the input data of Tables 1-2. It is shown from Fig. 3(a) that the breech position possesses the highest pressure in the chamber. The chamber pressure builds up as the propellant charge continue to burn then it decreases as the guided projectile moves down the bore. The ignition wave direction of propagation through the stick propellant charge as well as the wave front is clearly represented in Fig. 3(b). With the projectile motion the gas temperature is slowly decreases.

Most of propellant charge is ignited at time about 1.89 ms as it holds propellant surface temperature of about 615 K. The volume of the solid propellant decreases with the burning process, as shown in Fig. 3(c). It is observed in Fig. 3(d) that there is a region of negative velocity values in the early stage of ignition. The major reason of these negative velocities is; the tendency of gas phase combustion products to propagate towards the breech and the projectile base due to pressure gradient inside gun chamber, but due to the high inertia of solid-phase particles it have a lower velocities than that of the gas-phase.

5.2 Comparison between stick and 19-P propellant grains

Table 3 represents the comparisons between the maximum chamber pressure and projectile muzzle velocity of the simulation results of stick propellant and the experimental results of 19-P propellant charge [3-9].

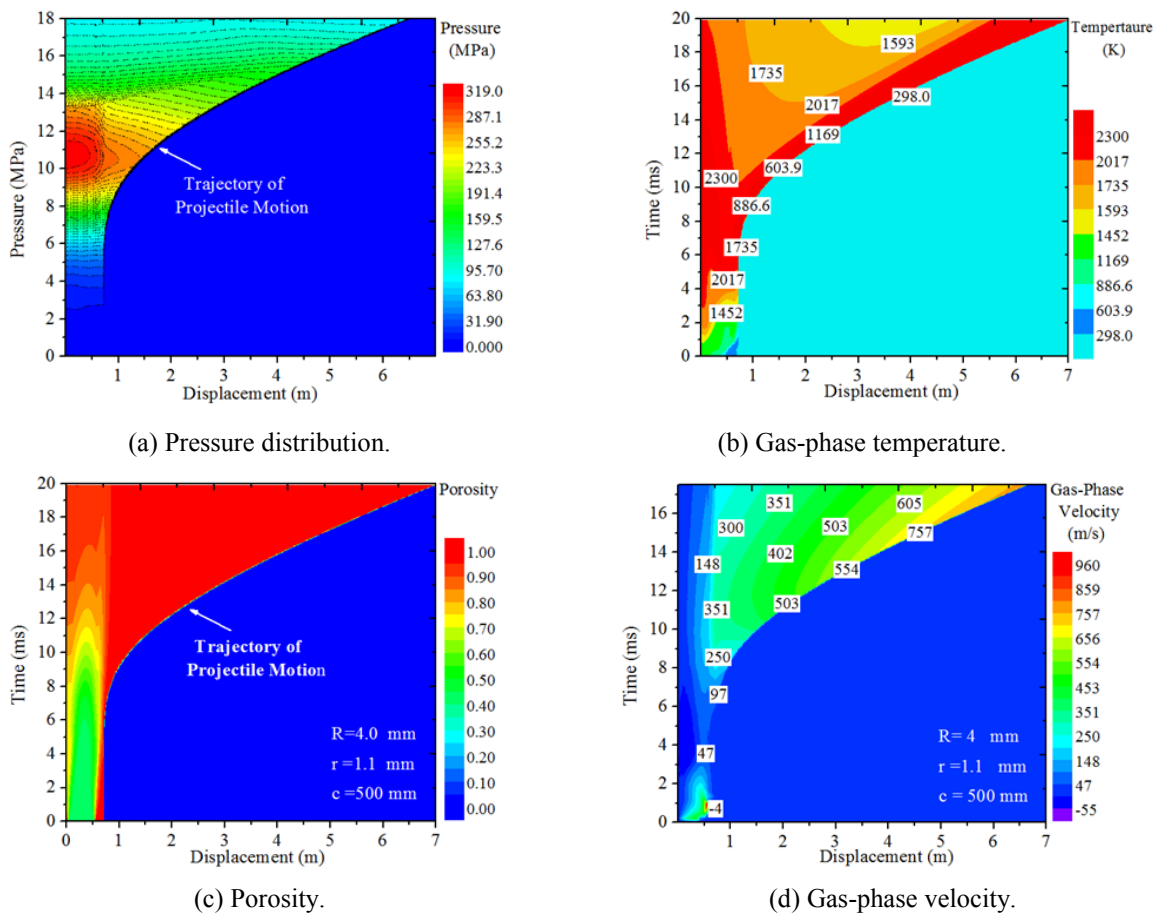


Fig. 3 Calculated z-t diagram of physical variables in large caliber conventional gun utilizing a stick propellant charge ($c = 500mm$, $R = 4mm$ and $r = 1.1mm$).

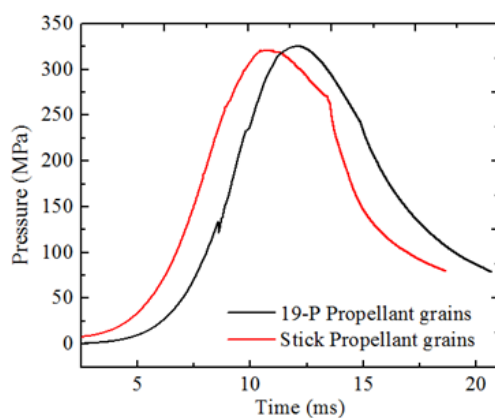
The simulation is carried out using the input data presented in Table 2 at stick propellant grain conditions of; $c = 500\text{mm}$, $R = 4\text{mm}$ and $r = 1.1\text{mm}$. Figure 4 represents the breech pressure histories and the differential pressure between the breech and the guided projectile base. For the same used amount of propelling charge (10.6 kg), it is revealed from Fig. 4(a) that the maximum pressure inside the gun chamber is almost the same for both stick and 19-P propellant grains. However, as shown in Fig. 4(b), the pressure waves marked a clear contrast in behavior. In case of 19-P grains, a rarefaction wave at time 5.8ms followed by strong shockwave at time 10.2ms disturbed the projectile base. These pressure fluctuations are considered as a severe disadvantage for this type of charges to launch a guided projectile from a conventional gun.

Conversely, the stick propellant configuration possess a lower pressure fluctuations than 19-P which assure more convenient and safe launching process for guided projectiles at the same interior ballistics conditions.

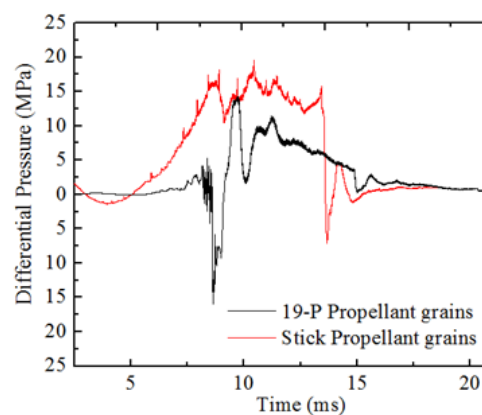
Figure 5 represents the guided projectile velocity-displacement time histories during the whole interior ballistics cycle. Due to its progressivity, high loading density and its low resistance to ignition flame propagation, the developed stick propellants grain configuration revealed an increase about 6.49% in muzzle velocity than 19-P grains for the same charge amount without an increase in the maximum chamber pressure. Also, it is shown from the figure that the projectile started to move in case of stick propellant charge at about 1.6ms earlier than in case of 19-P grains. This earlier movement can be to the pressure build up in the chamber due to the progressive burning behavior of stick propellant as well as the higher burn up mass and web thickness fractions than 19-P grains as shown in Fig. 6 .

Table 3 Comparisons between numerical results of stick propellant charge and experimental results of 19-P propellant charge.

Ballistic Parameter	Simulation results of stick propellant charge	Experimental Results of 19-P propellant charge
Maximum chamber pressure (MPa)	318.80	320.54
Muzzle velocity (m/s)	905.61	850.34



(a) Pressure history versus time.



(b) Pressure waves acting on projectile base.

Fig. 4. Pressure histories inside conventional gun tube using different propellant grain shapes.

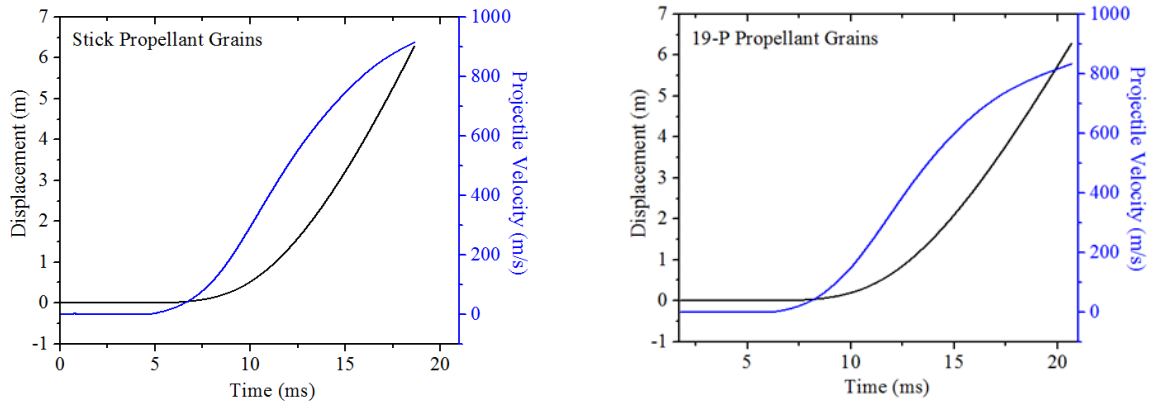


Fig. 5. Guided projectile velocity-displacement time histories inside conventional gun tube.

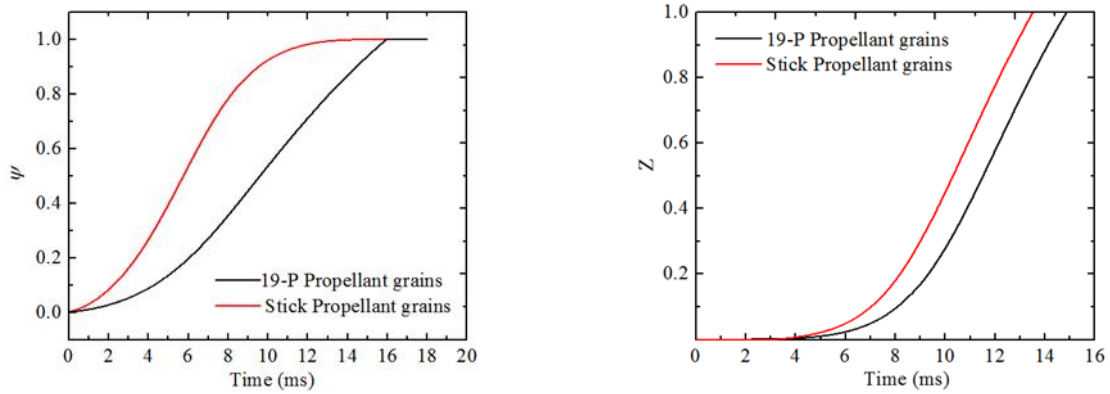


Fig. 6. Relative burned mass ψ and relative burned web thickness time histories for different propellant grain shapes.

5.3 Effects of stick grain size design parameters

In this research work, the different design parameters of stick propellant grains are changed to investigate its effects on maximum chamber pressure, pressure waves affecting on projectile base and guided projectile muzzle velocity. Figure 7 shows the time histories of pressure, projectile velocity, differential pressure between the breech position and the projectile base, and relative burned web thickness for three conditions of stick perforation radius r . The other dimensions of stick propellant grains as well as all the other interior ballistics working conditions are considered to be constant for all simulations. As shown in Fig. 7(a), large values of perforation radius of stick propellant grain leads to high chamber pressure and high muzzle velocity. The high burning rate of larger perforation radius r is due to the low resistance to the combustion flame propagation through the

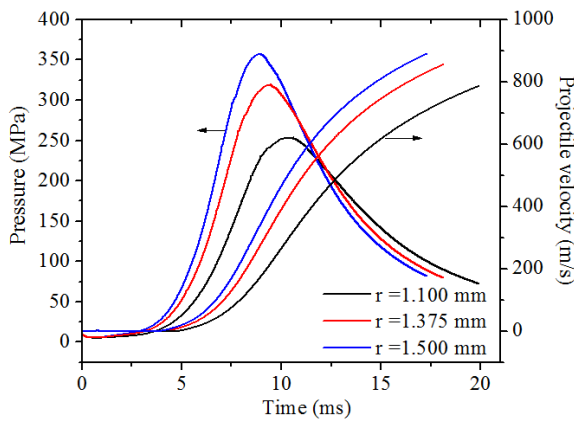
whole bundle of propellant. Therefore, the duration of the interior ballistic cycle is shorter in case of small values of r . The differential pressure has higher amplitudes in case of large values of r than the small values as shown in Fig. 7(c). These higher pressure wave values may affect the stability as well as the performance of guided projectile. It is also shown from Fig. 7(d) that for all conditions of perforation radius, the propellant is still burning in the chamber until the time of projectile ejection.

Figure 8 represents the time histories of pressure, guided projectile velocity, differential pressure between the breech position and the projectile base, and relative burned web thickness for three conditions of stick propellant radius R . As shown in Fig. 8(a), that the maximum chamber pressure possesses a high value in case of using stick propellant grain of smaller radius. This

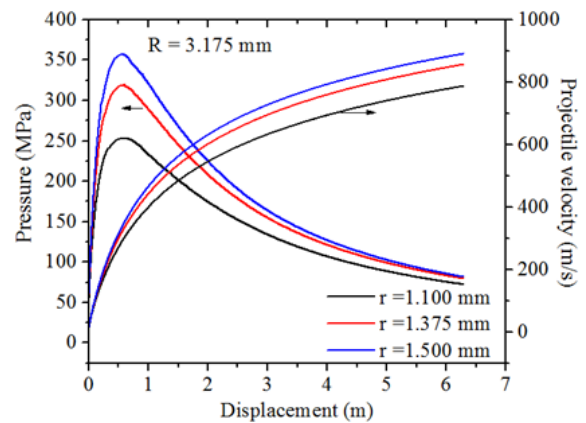
increase in pressure is related to the increased burned surface area of sharing propellant sticks as their number per propellant bundle is increased. Hence, the guided projectile acquires a high velocity value. However, the increase in the chamber pressure leads to high pressure wave fluctuations during the cycle as shown in Fig. 8(c). Vice versa, as the stick radius increase the maximum pressure decreases and the period from the ignition until the projectile exit the muzzle becomes larger than in case of small stick radius. Figure 7d shows that in case of the smallest perforation radius, the whole propellant charge is consumed and thus the total propellant chemical energy is exploited to launch the guided projectile, except some losses to the system.

Hence, the stick radius is required to be optimized to support a moderate maximum chamber pressure and as high as projectile muzzle velocity.

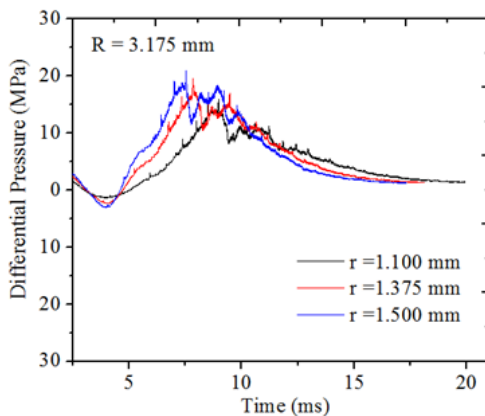
Figure 9 shows the effect of changing the stick propellant grain length on the maximum chamber pressure of the launch system and the projectile velocity. As the length of the stick grain increases, the maximum pressure and muzzle velocity increase as shown in Fig. 9(a) and Fig. (b). This increase is depending on the burning surface area. However, as shown in Fig. 9(c), the pressure fluctuations recorded a sharp change in case of long stick grains which. As shown in Fig. 9(d), even at these high pressure rates, there is a part of propelling charge still unburned inside the gun tube.



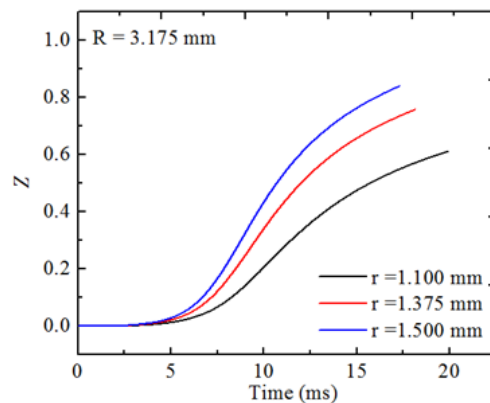
(a) Time histories of pressure and projectile velocity.



(b) Pressure and projectile velocity versus distance.

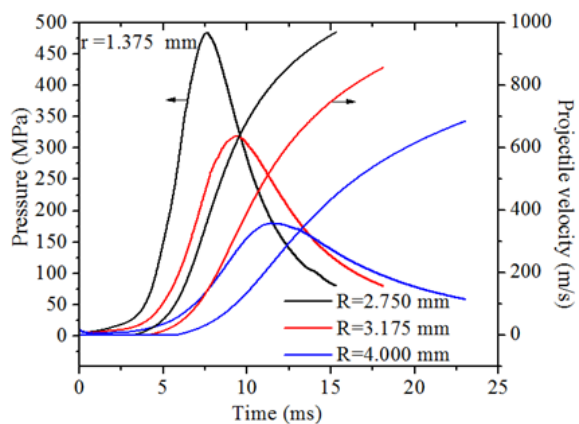


(c) Time histories of differential pressure.

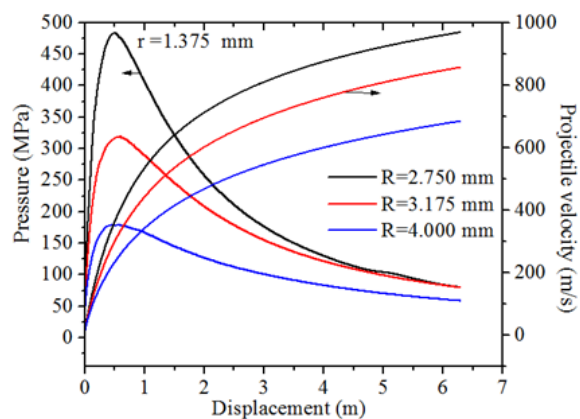


(d) Time histories of relative burned web thickness.

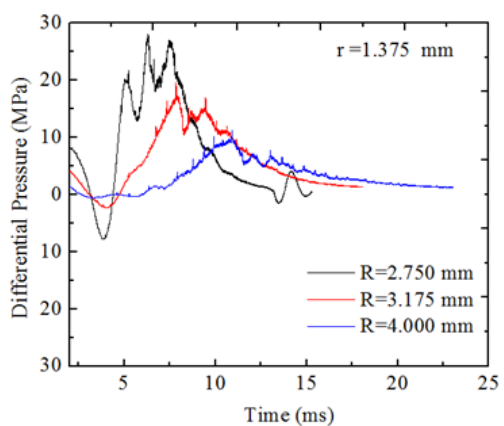
Fig. 7. Effect of changing stick propellant perforation diameter, r , on interior ballistics performance.



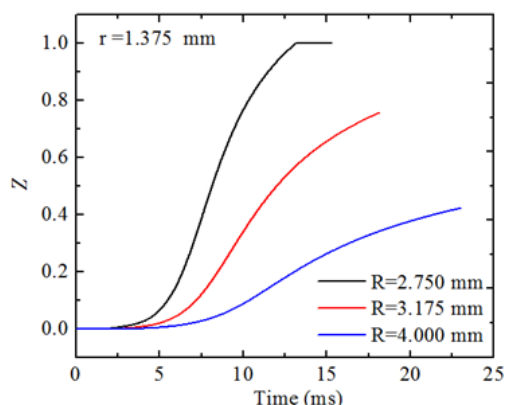
(a) Time histories of pressure and projectile velocity.



(b) Pressure and projectile velocity versus distance.

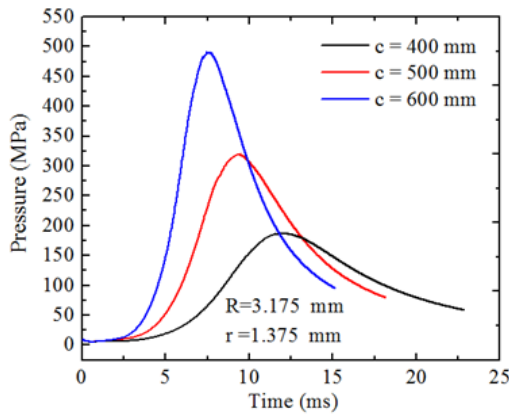


(c) Time histories of differential pressure.

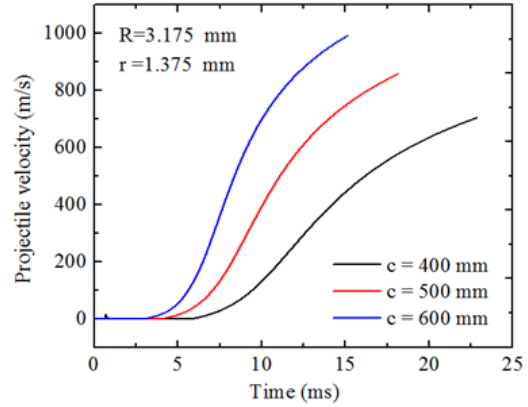


(d) Time histories of relative burned web thickness.

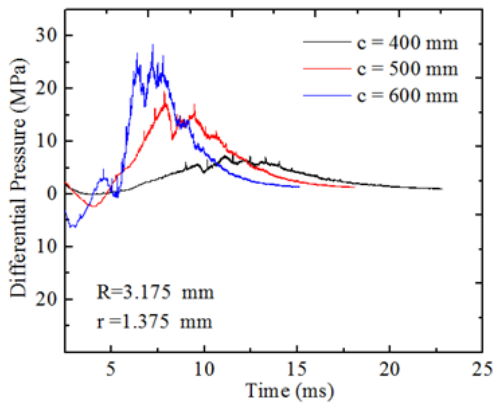
Fig. 8. Effect of changing stick propellant diameter, R , on interior ballistics performance.



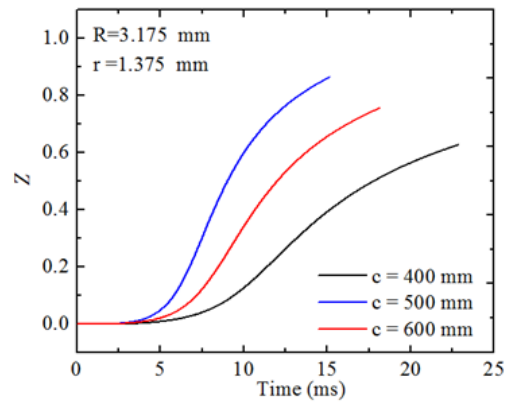
(a) Time histories of pressure



(b) Time histories of projectile velocity



(c) Time histories of differential pressure.



(d) Time histories of relative burned web thickness.

Fig. 9. Effect of changing stick propellant length, c , on interior ballistics performance.

6 Conclusions

The main objective of this research is to design a proper propellant charge via predicting the interior ballistics parameters such as chamber pressure and muzzle velocity to sustain accurate and safe launching process of guided projectiles employing conventional naval large caliber guns. Therefore, a two-phase fluid dynamics mathematical model of solid single-perforated stick propellant, and its products of combustion inside the gun tube during interior ballistics cycle is carried out. The main advantages of the developed model are; (1) predicting times and distributions of shock waves occurrence that can disturb the guided projectile during launching process, (2) estimating accurate

and fast interior ballistic parameters for conventional large caliber gun and (3) considered as a helpful tool for stick propelling charge design. The simulation results were compared with the experimental data that obtained from the previous work for granular propellant grains [3-9]. It was found that 19-P grains possess high pressure fluctuations which are considered a severe drawback for this type of charges to launch a guided projectile from conventional gun. It was obvious from the results that the stick propellant grain dimensions significantly affected the maximum chamber pressure and then the guided projectile muzzle velocity. Moreover, the results showed that the pressure wave's generation depends on the stick

propellant grain size parameters which have to be optimized for safe launching of guided projectile.

Acknowledgements

This work is supported by the Natural Science Foundation of Jiangsu Province (No.BK 20131348).

References

- [1]. P. G., Baer, and J.M., `Frankle, "The Simulation of Interior Ballistic Performance of Guns by Digital Computer Program", BRL, USA ARDC, Ballistic Research Laboratories, Aberdeen Proving Ground, MD, Report No. 1183., 1962
- [2]. K.D., Fickie, and J., Grosh, "A Technique for Code Augmentation. US Army Ballistic Research Laboratory, Aberdeen Proving Ground", MD, BRL-MR-3622, 1987.
- [3]. M. M., Rashad, X. B., Zhang, and H. Elsadek, "Numerical Simulation of Interior Ballistics for Large Caliber Guided Projectile Naval Gun", *J. of Eng. and Appl. Science*, Vol.60, No. 2 , 2013.
- [4]. C., Cheng, and X. B., Zhang," Modeling of Interior Ballistic Gas-Solid Flow Using a Coupled Computational Fluid Dynamics-Discrete Element Method", *J. of Applied Mechanics*, Vol. 80, No.3, 2013, pp. 031403.
- [5]. M. M., Rashad, X. B., Zhang, H., Elsadek, and C., Cheng, "Two-Phase Flow Interior Ballistics Model of Naval Large Caliber Guided Projectile Gun System", *Appl. Mech. and Materials*, Vol. 465-466, 2013, pp. 592-596.
- [6]. Cheng, C., Zhang, X. B., Rashad, M. M., and H. Elsadek," Study on multi-phase combustion based on high resolution approximate Riemann solver in guns", *J. of Ballistics*, Vol. 25, No.3, 2013, pp.79-82.
- [7]. C.J., Ma, and X.B., Zhang, "Simulation of Contamination Prevention for Optical Window in Laser Ignition Systems of Large-Caliber Guns", *ASME J. Appl. Mech.*, Vol. 78, No.5, 2011, pp. 051014.
- [8]. C., Cheng and X.B. Zhang "Numerical simulation of two-phase reactive flow with moving boundary." *Int. J. of Numerical Methods for Heat and Fluid Flow*, Vol. 23, No. 8, 2013, pp. 1277-1290.
- [9]. H. Q., Li, X.B., Zhang, Li, X. F., Elsadek, H. and Rashad, M. M., "Numerical simulation of laser ignition process based on photoacoustic effect." *J. of Nanjing University of Science and Technology*, Vol. 37, No. 5, 2013, pp.725-728.
- [10]. K. K., Kuo, K. C., Hsieh, and M. M., Athavale,"Modeling of Combustion Process of Stick Propellants via Combined Eulerian-Lagrangian Approach." *National Aeronautics and Space Administration*, Vol. 89, 1988, pp.181-194.
- [11]. J.M., Char, and K. K., Kuo," Study of Combustion Process of Single-Perforated Stick Propellants", *J. of propulsion and Power*, Vol. 5, no.3, 1989, pp.262-268.
- [12]. M., Hiroaki, M., Akiko, and N., Yuichi, "Numerical Prediction of Interior Ballistics Performance of Projectile Accelerator Using Granular or Tubular Solid Propellant", *Propellants Explos. Pyrotech.*, Vol. 38, 2013, pp.204 – 213.
- [13]. W. H., Albert, E. K., George, and S. G., Paul, "New Directions in Multiphase Flow Interior Ballistic Modeling", BRL Report No. 3102, *USA ARDC, Ballistic Research Laboratories*, Aberdeen Proving Ground, MD,1990.
- [14]. F. W., Robbins, and A. W., Horst, "A Simple Theoretical Analysis and Experimental Investigation of Burning Processes for Stick Propellant", *Proceedings of the 18th JANNAF Combustion Meeting*, CPIA Publication, Vol.347, No.2, pp. 1981, pp. 25-34.
- [15]. F. W., Robbins, J. A., Kudzal, J.A., McWilliams, and P.S., Gough, "Experimental Determination of Stick Charge Flow Resistance", *Proceedings of the 17th JANNAF Combustion Meeting*, CPIA Publication, Vol.329, No.2, 1980, pp.97-118.
- [16]. K. K., Kenneth,"Principles of combustions", Second Edition, John Wiley & Sons Inc., 2005, pp. 601-620.
- [17]. V. F., Baibuz, V. Yu., Zitserman, L. M., Golubushkin and I. G. Malyshev, "The Covolume and Equation of State of High-Temperatural Gases", *Translated from Inzhenerno-Fizicheskii Zhurnal*, Vol. 51, 1986, pp. 273-275.
- [18]. J.D., Anderson, "Computational fluid dynamics: The basics and applications", McGraw-Hill, New York, 1995, pp.320-345